Author/s:
Juillard, F;Bazot, Q;Mure, F;Tafforeau, L;MacRi, C;Rabourdin-Combe, C;Lotteau, V;Manet, E;Gruffat, H

Title:
Epstein-Barr virus protein EB2 stimulates cytoplasmic mRNA accumulation by counteracting the deleterious effects of SRp20 on viral mRNAs

Date:
2012-08-01

Citation:
Juillard, F., Bazot, Q., Mure, F., Tafforeau, L., MacRi, C., Rabourdin-Combe, C., Lotteau, V., Manet, E. & Gruffat, H. (2012). Epstein-Barr virus protein EB2 stimulates cytoplasmic mRNA accumulation by counteracting the deleterious effects of SRp20 on viral mRNAs. Nucleic Acids Research, 40 (14), pp.6834-6849. https://doi.org/10.1093/nar/gks319.

Persistent Link:
https://hdl.handle.net/11343/248220

6834–6849 *Nucleic Acids Research, 2012, Vol. 40, No. 14* *Published online 13 April 2012*
doi:10.1093/nar/gks319

Epstein–Barr virus protein EB2 stimulates cytoplasmic mRNA accumulation by counteracting the deleterious effects of SRp20 on viral mRNAs

Franceline Juillard[1,2,3], Quentin Bazot[1,2,3], Fabrice Mure[1,2,3], Lionel Tafforeau[3,4], Christophe Macri[1,2,3], Chantal Rabourdin-Combe[3,4], Vincent Lotteau[3,4], Evelyne Manet[1,2,3,*] and Henri Gruffat[1,2,3,*]

[1]INSERM U758, Unité de Virologie Humaine, 69364 Lyon, France, [2]Ecole Normale Supérieure de Lyon, 69364 Lyon, France, [3]Université de Lyon, 69361 Lyon, France and [4]INSERM U851, IMAP Team, 69365 Lyon, France

Received January 4, 2012; Revised March 19, 2012; Accepted March 23, 2012

ABSTRACT

The Epstein–Barr Virus (EBV) protein EB2 (also called Mta, SM and BMLF1), is an essential nuclear protein produced during the replicative cycle of EBV. EB2 is required for the efficient cytoplasmic accumulation of viral mRNAs derived from intronless genes. EB2 is an RNA-binding protein whose expression has been shown to influence RNA stability, splicing, nuclear export and translation. Using a yeast two-hybrid screen, we have identified three SR proteins, SF2/ASF, 9G8 and SRp20, as cellular partners of EB2. Then, by using siRNA to deplete cells of specific SR proteins, we found that SRp20 plays an essential role in the processing of several model mRNAs: the Renilla luciferase reporter mRNA, the human β-globin cDNA transcript and two EBV late mRNAs. These four mRNAs were previously found to be highly dependent on EB2 for their efficient cytoplasmic accumulation. Here, we show that SRp20 depletion results in an increase in the accumulation of these mRNAs, which correlates with an absence of additive effect of EB2, suggesting that EB2 functions by antagonizing SRp20. Moreover, by using RNA-immunoprecipitation assays we found that EB2 enhances the association of SRp20 with the β-globin transcript suggesting that EB2 acts by stabilizing SRp20's labile interactions with the RNA.

INTRODUCTION

In eukaryotic cells, nuclear export of mRNAs is mediated by conserved proteins which coat the nascent RNA co-transcriptionally to form export-competent mRNPs that are capped at their 5′-end, spliced, and cleaved/polyadenylated at their 3′-end [for a review, see (1)]. Translocation of mRNPs through the nuclear pore complex requires binding of a heterodimer composed of NXF1 and NXT1 (respectively Mex67 and Mtr2 in *Saccharomyces cerevisiae*), which escorts competent mRNPs out of the nucleus via direct interactions with nucleoporins lining the nuclear pore. Because of its low affinity for binding mRNAs, the heterodimer NXF1:NXT1 requires adaptator proteins, amongst which the best characterized is REF (2). In higher eukaryotes the recruitment of NXF1:NXT1 to mature mRNAs appears to be dependent upon 5′-cap addition and splicing. Two multiprotein complexes are known to be recruited as a consequence of splicing: the exon–junction complex (EJC) which is deposited 20–24 nt upstream of the exon–exon junction during splicing and which is associated with nonsense-mediated mRNA decay (NMD), and the human transcription/export complex (hTREX). hTREX contains the hTHO-complex (composed of hHpr1, hTho2, fSAP79, fSAP35 and fSAP24) associated with the RNA helicase UAP56 and the adaptator protein REF. Recent studies strongly suggest that the cap-binding protein CBP80 and factors deposited at the first exon–exon junction by splicing, cooperate to recruit hTREX onto spliced mRNAs (3). The presence of REF in this complex is

*To whom correspondence should be addressed. Tel: +33 472 728 955; Fax: +33 472 728 137; Email: henri.gruffat@ens-lyon.fr
Correspondence may also be addressed to Evelyne Manet. Tel: +33 472 72 81 76; Fax: +33 472 72 80 80; Email: evelyne.manet@ens-lyon.fr

The authors wish it to be known that, in their opinion, the first three authors should be regarded as joint First Authors.

thought to stimulate the recruitment of NXF1 onto the mRNPs and lead to their efficient export through the nuclear pore.

For mRNAs generated from intronless genes, two export pathways have been described. One implicates binding of SR proteins 9G8 and SRp20 to mRNAs (4). Similarly to REF, these two shuttling SR proteins have been found to serve as RNA-binding adaptors for NXF1 (5). The other pathway implicates recruitment of REF at the 5′-end of the mRNA by the cap-binding protein CBP20 (6).

In contrast to the majority of mammalian genes, most herpesvirus early and late genes are intronless. The efficient cytoplasmic accumulation of most of these intronless viral mRNAs appears to be strictly dependent on a viral gene product that shares properties with known mRNA export adaptors. The most studied of these factors are the herpes simplex virus type 1 (HSV1) protein ICP27 (7,8), the cytomegalovirus (CMV) protein UL69 (9), the Kaposi's sarcoma-associated herpes virus (KSHV) protein ORF57 (10,11), the herpes virus saimiri (HVS) protein ORF57 (12), the Varicella-Zoster virus (VZV) protein IE4 (13) and the Epstein–Barr virus (EBV) protein EB2 (also known as BMLF1, SM and Mta) (14,15). The EB2 protein of EBV is absolutely required for production of infectious viral particles (16). It binds RNA *in vitro* and *in vivo* via an arginine-rich region (17) and induces the cytoplasmic accumulation of most early and late viral mRNAs (16,18,19) both by interacting with cellular adaptators of the NXF1/NXT1 receptor pathway such as REF (20) or OTT1/RBM15 and OTT3/RBM15b (21), two RNA-binding proteins that belong to the human Spen (split end) protein family (22,23), and by directly interacting with NXF1 (24). Like cellular mRNA export factors, EB2 shuttles between the nucleus and the cytoplasm (14,20,24) and we have recently shown that it associates with polyribosomes and strongly stimulates translation of its target mRNAs (25). Moreover, it has recently been shown that EB2/SM modulates splice site selection of the host-cell STAT1 pre-mRNA by directly interacting with the cellular splicing factor SRp20 (26,27)

In order to better understand the mechanisms involved in the multiple functions of EB2, both in viral mRNA processing and translation, we used a wide yeast two-hybrid screen to identify the principal interactions of EB2 with the cellular proteome. Interestingly, we found specific interactions with three members of the SR protein family: SF2/ASF (SRSF1), SRp20 (SRSF3) and 9G8 (SRSF7). The SR protein family comprises a number of phylogenetically conserved and structurally related proteins. They have a common organization with the presence of one or two RNA recognition motifs (RRMs) at their N-termini that provide RNA-binding specificity, and a domain rich in arginine and serine dipeptides, termed the RS domain, at their C-termini. SR proteins have specific, yet degenerate RNA-binding sites. They were originally identified due to their activities as constitutive and alternative pre-mRNA splicing factors [for a review see (28,29)]. However, a subset of SR proteins, which includes SF2/ASF, SRp20 and 9G8, has been found to play additional roles in RNA processing. For example, SF2/ASF has been implicated in mRNA translation of an ESE (exonic splicing enhancer)-containing luciferase reporter (30,31), SRp20 has been shown to function in IRES (internal ribosome entry site)-mediated translation of viral RNA (32) and 9G8 in translation of un-spliced mRNA containing a CTE (constitutive transport element) (33). Moreover, SRp20 and 9G8 have been found to function in the nucleocytoplasmic export of mRNA by interacting with the mRNA nuclear export factor NXF1 (4,5).

After confirming the interactions found in the two-hybrid screen between EB2 and the three SR proteins by GST–pull-down and co-immunoprecipitation assays, we have studied the impact of depletion of these SR proteins from cells for the EB2-dependent cytoplasmic accumulation of two model transcripts generated from intronless reporter genes as well as two late viral mRNAs and virus particle production. Our results have led us to propose a new mechanism by which a viral protein enhances mRNA accumulation by antagonizing the action of SR proteins.

MATERIALS AND METHODS

Human lymphoblastoid cell cDNA library

Human peripheral blood mononuclear cells (PBMC) were freshly isolated by density-gradient centrifugation using Ficoll Hypaque (Sigma). B cells were purified from the PBMCs using anti-CD19 coated nanoparticules (EasySep, Stem Cell Technologies). Purified B cells were infected with a recombinant EBV expressing GFP as previously described (34) and infected cells were selected by hygromycin treatment. After several weeks in culture the resulting immortalized cells were used to generate a cDNA library in pACT2-GW (Invitrogen) (1.33×10^7 primary clones).

Plasmids

ORFs for full-length EB2, EB2Nter (amino acids 1–184) and EB2Cter (amino acids 185–479) were cloned in a Gateway recombinational cloning system (35) and deposited in a viral ORF repository, viralORFeome (36). Each ORF was PCR-amplified (with KOD polymerase, Novagen) using *attB1* and *attB2* recombination sites fused to forward and reverse primers, then cloned into pDONR207 (BP Clonase, Invitrogen). The ORFs were subsequently transferred (LR Clonase, Invitrogen) into the bait vector, pGBKT7, to be expressed as Gal4-DB fusions in yeast. Plasmids pCI-FlagEB2, pCI-FlagEB2Nter, pCI-FlagEB2Cter, pCI-FlagEB2 M1.2, pCI-FlagEB2Nter M1.2, pGEX-EB2Nter and pGEX-EB2Cter have been previously described (20,37). pGEX-SRp20, pGEX-9G8, pGEX-SF2/ASF have also been previously described (13). pGEX-SRp20 RRM was constructed by insertion of a stop codon at position 104 in pGEX-SRp20 by site-directed mutagenesis (QuickChange Site-Directed Mutagenesis kit, Stratagene). pGEX-SRp20 RS was generated by cloning a PCR-amplified SRp20 fragment into the pDEST15 vector (Invitrogen) using Gateway technology (Invitrogen). pDEST-MycNXF1 was generated by cloning a PCR-amplified fragment

into the pDEST-Myc vector (Invitrogen) using Gateway technology (Invitrogen). Expression plasmids for HA-SRp20, V5-SRp20, V5-9G8 and V5-SF2/ASF have been previously described (13) as well as plasmid pcDNAGlobinRen (25). Plasmids β1(−)2(−), 1X-βG, 2X-βG and 4X-βG were a kind gift from Dr Y. Huang. Plasmid pCI-FlagBFRF3-i has been previously described (18). Plasmid pCI-FlagBDLF1-i was constructed in a similar way to pCI-FlagBFRF3-i.

Yeast two-hybrid screens

The screens were performed by yeast mating using the AH109 and Y187 yeast strains (Clontech) (38,39). Bait vectors, pGBKT7-EB2, pGBKT7-EB2Nter, pGBKT7-EB2Cter were transformed into AH109 (bait strain), and the human lymphoblastoid cell line AD–cDNA library was transformed into Y187 (prey strain). Single bait strains were mated with prey strain and then diploids were plated on SD-W-L-H + 5 mM 3-AT medium. Positive clones were maintained on this selective medium for 15 days to eliminate any contaminating AD–cDNA plasmid (40). AD–cDNAs were amplified by colony PCR and inserts were sequenced and identified by automatic BLAST as previously described (41). All primary positive clones were then retested in fresh yeast: bait vectors were retransformed in the AH109 strain and PCR-amplified prey cDNA (for each identified putative interactor) was transformed in the Y187 strain in combination with linearized pACT2 prey vector [gap repair (42)]. All prey strains were then mated with the different bait strains in an 'all against all' fashion, generating a Y2H pairwise matrix.

Cell culture and transfections

HeLa cells and HEK293T cells were grown at 37°C in DMEM supplemented with 10% Foetal Bovine Serum (FBS) and penicillin–streptomycin. HEK293 cells infected with the recombinant EBV virus ($HEK293_{EBV}$), a gift from Dr W. Hammerschmidt, have been described previously (43). The recombinant virus encodes Green Fluorescent Protein (GFP) and the hygromycin B resistance gene. $HEK293_{EBV\text{-}BMLF1KO}$ has been previously described (16). $HEK293_{EBV}$ and $HEK293_{EBV\text{-}BMLF1KO}$ cells were maintained in Dulbecco's modified Eagle medium (DMEM), supplemented with 10% FBS, penicillin–streptomycin and hygromycin B (100 μg/ml; Invitrogen). Raji cells were maintained in RPMI 1640 medium supplemented with 10% FBS and penicillin–streptomycin. Plasmid transfections were performed either by the calcium phosphate precipitate method or by using Lipofectamine 2000 (Invitrogen) following the manufacturer's protocol. siRNA were transfected by using INTERFERin (Polyplus Transfection) 48 h prior to DNA transfections. siRNA oligonucleotide sequences used are as follows: 5′-GGAAAUAGAAGACAGUUU G(dT)(dT)-3′ and antisense for the SRp20 siRNA (32); 5′-AGGAGAGUUAGAAAGGGCU(dT)(dT)-3′ and antisense for the 9G8 siRNA (44); 5′-CCAAGGACAU UGAGGACGU(dT)(dT)-3′ and antisense for the SF2/ASF siRNA (44). Firefly luciferase siRNAs were used as a control.

Virus production and titration

$HEK293_{EBV}$ cells or $HEK293_{EBV\text{-}BMLF1KO}$ cells were transfected with pCMV-BZLF1, an expression vector coding for the EBV transcriptional activator EB1 (also called Zta or Zebra), to activate the EBV productive cycle. Supernatants from transfected cells were harvested at 48 h post-transfection and filtered through a 0.45 -μm pore size filter. Raji cells (1×10^5) were incubated in 0.5 ml of virus solution for 6–8 h at 37°C in a 24-well plate. Cells were then washed, re-suspended in 1 ml of RPMI and incubated for an additional 72 h at 37°C. GFP-expressing Raji cells were quantified by FACS analysis.

Co-immunoprecipitation assays and western blots

Transfected HEK293T cells were harvested from 100-mm dishes 48 h post-transfection and lysed in IP buffer (50 mM Tris–HCl pH 7.5, 150 mM NaCl, 1 mM EDTA, 1 mM DTT and 0.5% Nonidet P-40) plus protease inhibitors (Roche Molecular Biochemicals) and phosphatase inhibitors (Phosphatase Inhibitor Cocktail 2, Sigma-Aldrich). For immunoprecipitation of the transiently expressed F.EB2 protein, cell extracts were incubated with 30 μl anti-Flag M2 affinity gel (Sigma) for 4 h at 4°C and immunopurified proteins were analysed by western blotting. Antibodies used for western blotting analysis were an anti-Flag rabbit polyclonal antibody (Sigma), an anti-V5 rabbit polyclonal antibody (Sigma), an anti-SRp20 mAb (clone 7B4, Invitrogen), an anti-9G8 rabbit polyclonal antibody (Sigma), an anti-SF2/ASF mAb (clone 96, Invitrogen) and an anti-α-Tubulin mAb (B-5-1-2, Sigma). The appropriate anti-mouse or anti-rabbit horseradish peroxidase (HRP)-conjugated antibodies (GE healthcare) were used as secondary antibodies. Myc-tagged proteins were revealed using a c-Myc (9E10) HRP-conjugated antibody (Santa Cruz). RNase treatment was performed by adding 2 μl of RNase A (10 mg/ml) to each reaction. Western blots were revealed using ECL (Pierce).

In vitro GST pull-down assays

GST and GST-fusion proteins were purified from *Escherichia coli* BL21 (DE3) codon plus strain extracts, with glutathione–Sepharose 4B beads (Amersham Biosciences). Beads carrying the GST or the GST-fusion proteins were equilibrated in TNTB-binding buffer (10 mM Tris–HCl pH 8, 250 mM NaCl, 0.1% NP40 and 2 mg/ml BSA) in the presence of protease inhibitors (complete EDTA-free cocktail from Roche Molecular Biochemicals) and incubated with radiolabelled proteins synthesized *in vitro* in the presence of [^{35}S]-methionine using the TnT-Coupled Transcription/Translation system (Promega), in TNTB for 4 h at 4°C. RNase treatment was performed by adding 1 μl of RNase A (10 mg/ml) and 1 μl of RNase T1 (10 U/μl) in the incubation reaction. Beads were washed 5× in TNTB buffer without BSA and bound

proteins were fractionated by SDS–PAGE and revealed by autoradiography

Imunofluorescence assays

For indirect immunofluorescence experiments, an anti-Flag polyclonal antibody (Sigma) and an anti-HA mAb (Sigma) were used as primary antibodies. Alexa Fluor 488 goat anti-rabbit antibody (Invitrogen) and a Fluorolink Cy3-labelled goat anti-mouse IgG (H+L) (GE Healthcare) were used as secondary antibodies. Cell nuclei were stained by incubation with 5 μg/ml Hoescht 33258 (Sigma).

RT–PCR amplifications and RNA immunoprecipitations

RNA extractions, quantitative reverse transcription PCR (RT–qPCR) from nuclear and cytoplasmic RNAs were performed as previously described (25). For semi-quantitative RT–PCR, RNA was extracted using TRIzol (Invitrogen). Any contaminating DNA was removed from RNA samples using RQ1 DNase (Promega). RT–PCR was then performed using the qScript cDNA SuperMix from Quanta (RT) and GoTaq DNA polymerase (Promega) (PCR) in the presence of [α^{32}P]-dCTP. The following primer pairs were used to amplify the human β-globin mRNA: 5′-CATTTGCTTCTGACACAACTG-3′ and 5′-GCAGAATCCAGATGCTCAAGG-3′. β-actin, BDLF1 and BFRF3 PCR primers have been previously described (18,25). PCRs were performed on various amounts of the RT reaction mixtures to obtain a linearly increasing signal after 25 cycles. The number of PCR cycles used in all subsequent assays was 25. PCR fragments were analysed on 6% polyacrylamide gels and data were quantified by scanning the gels with a PhosphorImager. RNA immunoprecipitations were realized using the following protocol [modified from Boyne *et al.* (45)]. HeLa cells were washed with ice-cold PBS and UV-irradiated at 900 mJ/cm^2 in a Bio-Link crosslinker (Vilbert-Lourmat). Cells were scraped, transferred to an RNase-free tube and pelleted at 1200 rpm for 5 min. Cell pellets were re-suspended in 400 μl of TAP lysis buffer (10 mM HEPES, 10 mM KCl, 2 mM MgCl2, 0.5% Nonidet P-40, 5% glycerol, protease inhibitors [Roche Molecular Biochemicals), 1 μl/ml RNasin (Promega)]. Cells were incubated on ice for 30 min with occasional vortexing to lyse cells. For immunoprecipitations, protein A-Sepharose beads were prepared, coupled either to anti-SRp20 monoclonal antibody (Invitrogen) or anti-Flag M2 monoclonal antibody (Sigma). The antibody-coated beads were incubated with the cleared cell lysates for 4 h at 4°C. Beads were then washed 5× with NT2 buffer [50 mM Tris–HCl, pH 7.4, 150 mM NaCl, 1 mM MgCl2, 0.05% Nonidet P-40, 1 μl/ml RNasin (Promega)], and RNA was eluted by heating at 55°C for 15 min in 100 μl NT2 buffer containing 0.1% SDS and 0.5 μg/ml proteinase K. Beads were pelleted, and the supernatant transferred to a fresh RNase-free tube. RNA was then extracted and analysed as described above.

RESULTS

Identification of the three SR proteins, 9G8, SF2/ASF and SRp20 as specific interactors of the EBV EB2 protein in a yeast two-hybrid screen

We used the yeast two-hybrid (Y2H) system to identify cellular proteins that interact with EB2. Three constructs, encoding full length, N-terminal half (amino acids 1–184) or C-terminal half (amino acids 185–479) of EB2 were used to probe a human lymphoblastoid cell line (EBV-infected) cDNA library. Three independent screens were performed with each EB2-derived bait protein by mating. In total, each EB2 construct was screened against 2–8 × 10^7 human AD–Y fusion proteins and 269 clones (corresponding to 64 different putative interactions) were initially characterized following PCR amplification of the cDNAs and sequencing. The data set was retested by direct Y2H between EB2 protein baits and cellular protein preys identified by our Y2H screens (Y2H pairwise matrices). After elimination of autoactivators, 43 Y2H interactors were retested positive (Table 1). From the 269 initial positive colonies, 80 corresponded to an interaction of EB2 with itself via its C-terminal domain. In our list of cellular interactors, only *Sp100* (46) and *RBM15B* (21) have been previously described as direct interactors for EB2. A majority of the newly identified interactors corresponds to proteins involved in RNA metabolism. Among them, we found three members of the highly conserved SR protein family, namely 9G8 (*SFRS7*), SF2/ASF (*SFRS1*) and SRp20 (*SFRS3*). To confirm the interaction between EB2 and the three SR proteins in mammalian cells, we performed co-immunoprecipitation assays. V5-tagged 9G8, SF2/ASF, SRp20—or Myc-tagged NXF1 as a positive control—were expressed in HEK293T cells either alone or together with Flag-tagged EB2. Immunoprecipitations were performed using an M2 anti-Flag mAb affinity gel in the presence or absence of RNase and the immunoprecipitated complexes were analysed by western blotting. As published previously (24), NXF1 was efficiently co-immunoprecipitated with EB2 and the interaction was found to be drastically reduced in the presence of RNase (Figure 1D). Interestingly, 9G8 (panel A), SF2/ASF (panel B) and SRp20 (panel C) were all specifically co-immunoprecipitated with EB2 both in the presence or absence of RNase treatment indicating that all three SR proteins can interact with EB2 in mammalian cells and that these interactions are largely independent of the presence of RNA.

EB2 interacts with 9G8, SF2/ASF and SRp20 via its C-terminal domain

To confirm that EB2 interacts directly with the SR proteins and to identify the region of EB2 that is involved in each interaction, we performed *in vitro* binding assays by using GST fusion proteins produced in bacteria and ^{35}S-proteins that were *in vitro*-translated in reticulocyte lysates. In a first series of experiments, ^{35}S-labelled EB2, EB2Nter or EB2Cter (Figure 2A) were

Table 1. List of cellular proteins interacting with EB2 identified in the Y2H screen

NCBI GeneID	Nb of hits	Gene symbol	Full name
RNA metabolism			
6672	7	*SP100*	SP100 nuclear antigen
22827	9[a]	*PUF60*	Poly-U-binding splicing factor 60 kDa
8175	1	*SF3A2*	Splicing factor 3a, subunit 2, 66 kDa
6426	3[a]	*SRSF1*	Splicing factor, arginine/serine-rich 1
6432	1[a]	*SRSF7*	Splicing factor, arginine/serine-rich 7, 35 kDa
6428	10[a]	*SRSF3*	Splicing factor, arginine/serine-rich 3
8233	3	*ZRSR2*	Zinc finger (CCCH type), RNA-binding motif and serine/arginine-rich 2
3183	20[a]	*HNRNPC*	Heterogeneous nuclear ribonucleoprotein C (C1/C2)
29890	2[a]	*RBM15B*	RNA-binding motif protein 15B
Ribosome components			
6138	13	*RPL15*	Ribosomal protein L15
6129	1	*RPL7*	Ribosomal protein L7
6142	6	*RPL18A*	Ribosomal protein 18A
91582	2	*RPS19BP1*	Ribosomal protein S19-binding protein 1
7311	1	*UBA52*	Ubiquitin A-52 residue ribosomal protein fusion product 1
Transcriptional regulation			
10743	3	*RAI1*	Retinoic acid induced 1
30836	1	*DNTTIP2*	Deoxynucleotidyltransferase, terminal, interacting protein2
3663	8	*IRF5*	Interferon regulatory factor 5
Ubiquitination			
9636	3	*ISG15*	ISG15 ubiquitin-like modifier
7329	4	*UBE2I*	Ubiquitin-conjugating enzyme E2I (UBC9 homologue, yeast)
Others			
118881	3	*COMTD1*	Catechol-*O*-methyltransferase domain containing 1
8525	3	*DGKZ*	Diacylglycerol kinase ζ 104 kDa
7266	1	*DNAJC7*	DnaJ (Hsp40) homologue, subfamily C, member 7
4050	5	*LTB*	Lymphotoxin β (TNF superfamily member 3)
5155	8	*PDGFB*	sarcoma viral (v-sis oncogene homologue)
6643	2	*SNX22*	Sorting nexin 2
147	1	*ADRA1A*	Adrenergic receptor, α-1B-, receptor
Unknown function			
81844	2	*TRIM56*	Tripartite motif-containing 56
55661	24	*DDX27*	DEAD (Asp-Glu-Ala-Asp) box polypeptide 27
79009	1	*DDX50*	DEAD (Asp-Glu-Ala-Asp) box polypeptide 50
23518	2	*R3HDM1*	R3H domain containing 1
51111	1	*SUV420H1*	Suppressor of variegation 4–20 homologue 1 (*Drosophila*)
65265	1	*C8orf33*	Chromosome 8 open reading frame 33
84273	2	*C4orf14*	Chromosome 4 open reading frame 14
Zinc-finger proteins			
7738	1	*ZNF184*	Zinc-finger protein 184
63977	1	*ZNF298*	Zinc-finger protein 298
126295	2	*ZNF57*	Zinc-finger protein 57
10782	2	*ZNF274*	Zinc-finger protein 274
79759	1	*ZNF668*	Zinc-finger protein 668
163049	1	*ZNF791*	Zinc-finger protein 791
90987	1	*ZNF251*	Zinc-finger protein 251
55769	1	*ZNF83*	Zinc-finger protein 83
3104	1	*ZBTB48*	Zinc-finger and BTB domain containing 48
Viral protein			
5176227	80[a]	*EB2*	mRNA export factor EB2

[a]confirmed by coIP *in vivo*.
Each human gene is identified by its National Center for Biotechnology Information (NCBI) gene ID (first column), Gene symbol (third column) and full name (fourth column). The number of independent clones found in the Y2H screen for a given partner is indicated in the second column.

incubated with GST, GST–9G8, GST–SF2/ASF or GST–SRp20 proteins bound to Glutathione Sepharose beads in the presence of RNase. As shown in Figure 2B, EB2 was efficiently retained on GST–9G8, GST–SF2/ASF and GST–SRp20 but not on GST alone, which strongly suggests a direct interaction between EB2 and each of the three SR proteins. When we used the C-terminal half of EB2 (EB2Cter) we observed that this protein was retained on both GST–9G8 and GST–SRp20, but less efficiently on GST–SF2/ASF. On the contrary, the N-terminal domain of EB2 (EB2Nter) was not retained on GST–9G8 or GST–SRp20, but a weak interaction was detected with GST–SF2/ASF. In a reverse series of experiments, ^{35}S-labelled 9G8, SF2/ASF or SRp20 were incubated with GST, GST–EB2Nter or GST–EB2Cter (Figure 2C). All three proteins were retained on GST–EB2Cter, whereas interaction with GST–EB2Nter was either non-detectable (SRp20) or much

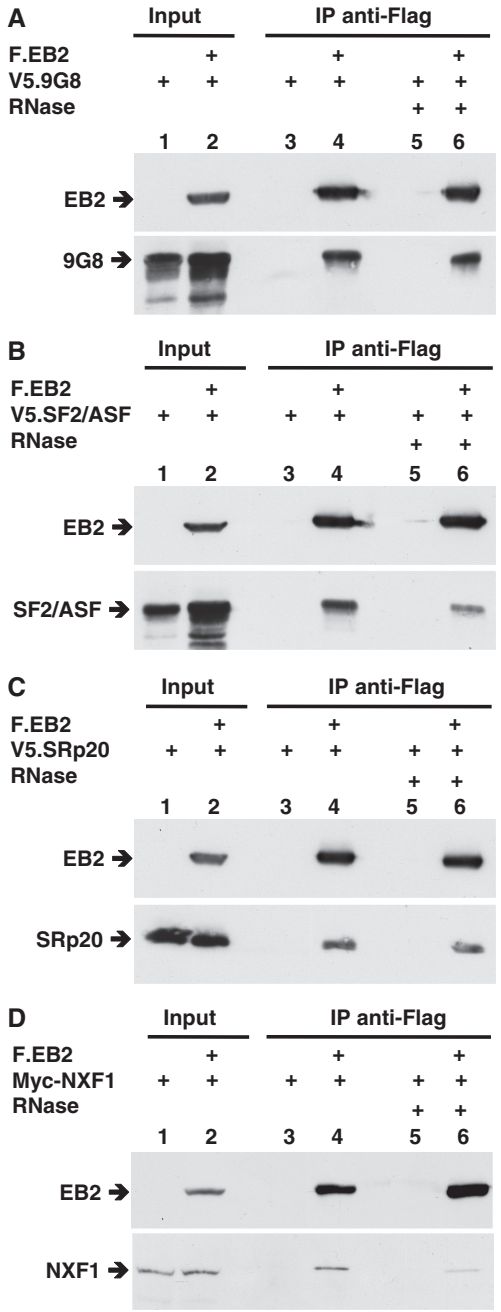

Figure 1. SRp20, 9G8 and SF2/ASF coimmunoprecipitate with EB2. V5-tagged 9G8 (**A**), V5-tagged SF2/ASF (**B**), V5-tagged SRp20 (**C**) or c-Myc-tagged NXF1 (**D**) were expressed by transient transfection in HEK293T cells either alone or together with Flag-tagged EB2. Lysates were prepared and immunoprecipitations performed using an M2 anti-Flag mAb affinity gel in presence or absence of RNAse. The immunoprecipitated complexes were then analysed by western blotting using an anti-Flag polyclonal antibody to visualize EB2, an anti-V5 polyclonal antibody to visualize 9G8, SF2/ASF and SRp20 or an anti-c-Myc monoclonal antibody for NXF1. The 'input' corresponds to 15% of the material present in the immunoprecipitated lysates.

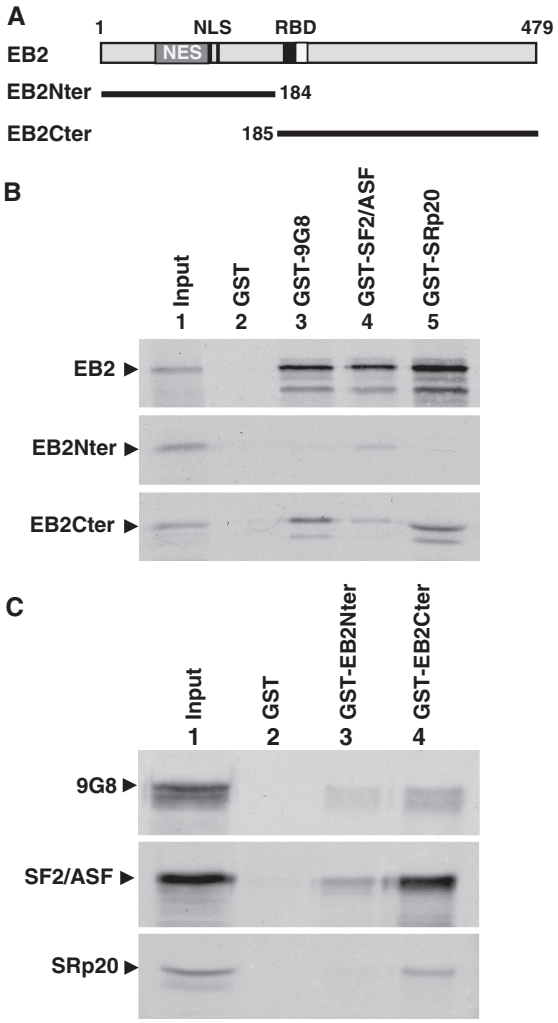

Figure 2. SRp20, 9G8 and SF2/ASF interacts with the C-terminal half of EB2 *in vitro*. (**A**) Schematic representation of the EB2 protein. The light gray box represents the nuclear export domain (NES) previously identified in the protein, the dark gray box, the RNA-binding domain (RBD), the white box, the REF interacting domain and the two vertical bars the Nuclear Localization Signals (NLS). Below, the C-terminal and N-terminal deletion mutants (EB2Nter and EB2Cter respectively) are represented. (**B**) ^{35}S-labelled EB2, EB2Nter or EB2Cter were incubated with purified GST, GST–9G8, GST–SF2/ASF or GST–SRp20 bound to glutathione sepharose beads. The bound proteins were analysed by SDS–PAGE and visualized by autoradiography. In lane 1, the equivalent of one-fifth of the EB2-, EB2Nter- or EB2Cter-expressing rabbit reticulocyte lysate used in each assay was loaded onto the gel. (**C**) ^{35}S-labelled 9G8, SF2/ASF or SRp20 were incubated with purified GST, GST–EB2Nter or GST–EB2Cter bound to glutathione sepharose beads. The bound proteins were analysed by SDS–PAGE and visualized by autoradiography. In lane 1, the equivalent of one-fifth of the 9G8-, SF2/ASF- or SRp20-expressing rabbit reticulocyte lysate used in each assay was loaded onto the gel.

weaker (9G8 and SF2/ASF). From these experiments we conclude that the main interaction domain between EB2 and the three SR proteins is located in its C-terminal half.

We then asked which domain of SRp20 was involved in the interaction with EB2. For this, we generated two GST–SRp20 mutant fusion proteins: one of the fusion protein carries the N-terminal RRM (RRM) domain, the other carries the RS-rich C-terminal domain (Figure 3A). The results (Figure 3B) suggest that the

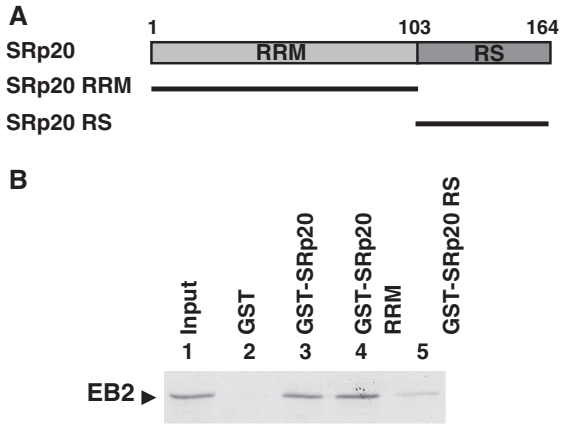

Figure 3. Mapping of the interaction domains of EB2 in SRp20. (**A**) Schematic representation of SRp20 and deletion mutants. (**B**) ^{35}S-labelled EB2 was incubated with purified GST, GST–SRp20, GST–SRp20 RRM or GST–SRp20 RS bound to glutathione sepharose beads. The bound proteins were analysed by SDS–PAGE and visualized by autoradiography. In lane 1, the equivalent of one-tenth of EB2-expressing rabbit reticulocyte lysate used in each assay was loaded onto the gel.

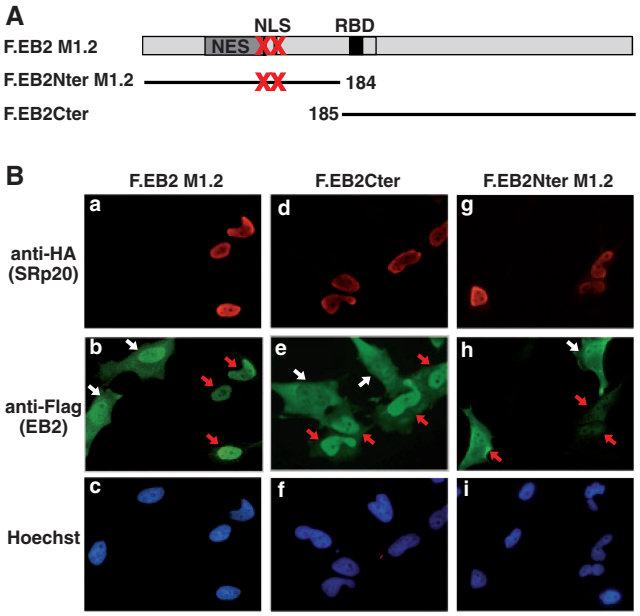

Figure 4. SRp20 over-expression induces retention of an NLS-deficient EB2 protein in the nuclei of HeLa cells. (**A**) Schematic representation of EB2 and EB2 mutants. (**B**) HeLa cells were co-transfected with expression vectors for HA-SRp20 and either FlagEB2 M1.2, FlagEB2Cter or FlagEB2Nter M1.2. Proteins were visualized by indirect immunofluorescence using an anti-HA mAb (for detection of HA-SRp20) (panels a, d and g) and an anti-Flag polyclonal antibody (for detection of FlagEB2 protein and mutants as indicated) (panels b, e and h). An Alexa Fluor 488 goat anti-rabbit antibody and a Fluorolink Cy3-labelled goat anti-mouse IgG (H+L) antibody were used as secondary antibodies respectively. Cell nuclei were stained with Hoechst 33258 (Sigma) (panels c, f and i). Red arrows indicate cells in which SRp20 is over-expressed together with FlagEB2 (or mutant FlagEB2) whereas white arrows indicate cells in which FlagEB2 (or mutant proteins) is expressed but SRp20 is not over-expressed.

interaction domain of SRp20 with EB2 is located within the first 103 amino acids, which corroborates the finding of Verma *et al.* (27).

Over-expression of SRp20, 9G8 and SF2/ASF induces the nuclear re-localization of cytoplasmic EB2 mutant derivatives

Although SRp20 has been previously described as a shuttling protein, it is mostly detected in the nucleus. EB2—also a shuttling protein—is similarly predominantly found at steady state in the nucleus and we have previously characterized two nuclear localization signals of the protein in its N-terminal half: an EB2 protein with its first 184 amino acids deleted was mostly cytoplasmic. Furthermore, by mutating two sequences—KRRR (NLS1: amino acids 126–130) and KRR (NLS2: amino acids 143–145)—to alanines, the resulting protein, F.EB2 M1.2 was found to be partially cytoplasmic (20). We made use of these EB2 cytoplasmic mutants to ask whether over-expression of nuclear SRp20 in HeLa cells would induce a re-localization of cytoplasmic EB2 mutants into the nucleus. We thus co-expressed HA-tagged SRp20 with each one of the three EB2 mutant proteins depicted in Figure 4A. The respective localization of the proteins was then visualized by immunofluorescence. As shown in Figure 4B, SRp20 was efficiently over-expressed only in a subset of the transfected cells (compare panels a, d and g to panels c, f and i respectively). Interestingly, when we compared the localization of F.EB2 M1.2 between cells over-expressing or not SRp20, we found that F.EB2 M1.2 became fully nuclear in cells over-expressing SRp20 (Figure 4B, panel b). In accordance with this, similar results were obtained when we used the F.EB2Cter protein. This protein, mostly cytoplasmic in cells that did not over-express SRp20, was clearly concentrated in the nuclei of cells over-expressing the SR protein (Figure 4B, panel e). In order to determine if the translocation of cytoplasmic EB2 into the nucleus was due to a direct interaction with SRp20, we used the F.EB2Nter M1.2 protein, which does not contain the SRp20 interaction domain. Again, due to the mutation of the two NLS sequences, the protein was mostly cytoplasmic. This cytoplasmic localization was not affected by the presence or not, of over-expressed SRp20 (Figure 4B, panel h). Similar results were obtained with both SF2/ASF and 9G8 (data not shown). Taken together, these experiments indicate that EB2 interacts with the three SR proteins within live cells.

Down-regulation of SRp20 expression by siRNA results in a strong inhibition of the EB2-dependent cytoplasmic Renilla luciferase mRNA accumulation

Since we previously reported that EB2 significantly increases the amount of cytoplasmic Renilla luciferase mRNA expressed from an intronless construct (25), we asked whether the SR proteins SRp20, 9G8 or SF2/ASF could play a role in the EB2-dependent cytoplasmic accumulation of this specific mRNA. The Renilla luciferase reporter construct pcDNAGlobinRen (Figure 5A) was thus transfected into HeLa cells, together or not, with

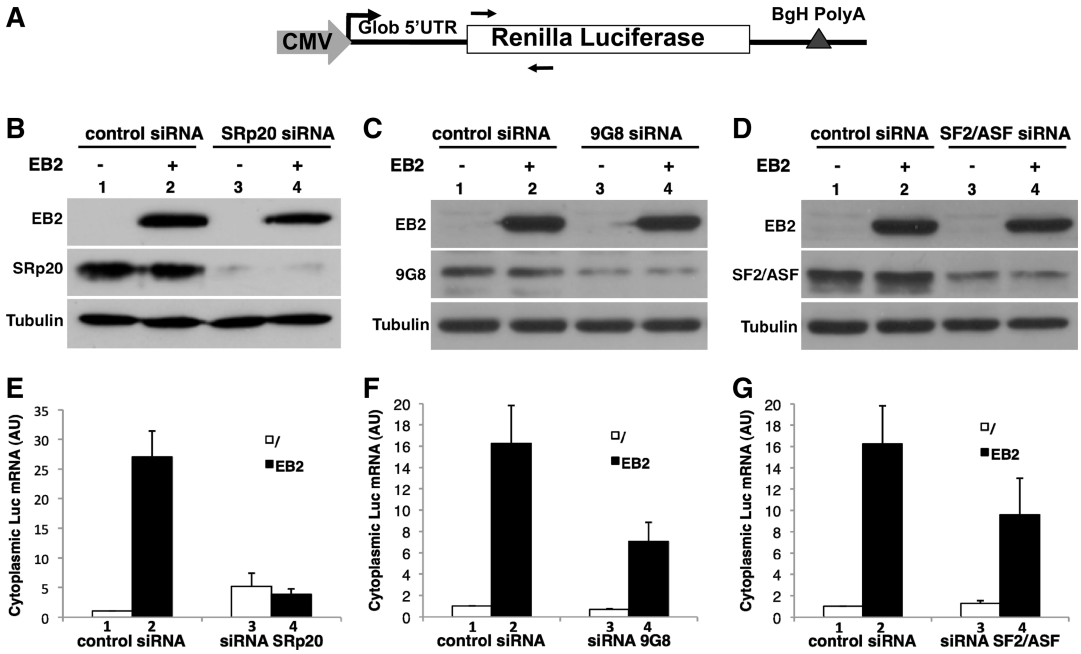

Figure 5. SRp20 is required for the EB2-dependent cytoplasmic accumulation of Renilla luciferase mRNA. (**A**) Schematic representation of the Renilla luciferase intronless-coding vector (pcDNAGlobinRen) showing positions of the CMV promoter and BGH polyadenylation signal. Small arrows indicate the position of the primers used for the PCR. (**B-D**) Immunoblots of HeLa cells co-transfected with pcDNAGlobinRen together with pCI-Flag EB2 as indicated in the figure. Cells were previously transfected with either a control siRNA (lanes 1 and 2 of each panel) or an siRNA specific for SRp20 (panel B, lanes 3 and 4), 9G8 (panel C, lanes 3 and 4) or SF2/ASF (panel D, lanes 3 and 4). The blots were either probed with an M2-Flag mAb to detect Flag-EB2, an anti-SRp20 mAb, an anti-9G8, an anti-SF2/ASF, or an anti-α-Tubulin as a control of total protein amounts. (**E–G**) Quantification of cytoplasmic luciferase encoding mRNAs by RT–qPCR using GAPDH as an internal control. mRNAs were extracted from cells transfected as described in B, C and D respectively. Experiments were made three times and the error bars represent standard deviations.

an expression plasmid for EB2 48 h after transfection of the cells with an siRNA specific for SRp20, 9G8, SF2/ASF or a control siRNA. Both the expression level of EB2 and the efficiency of SRp20, 9G8 or ASF/SF2 down-regulation by the specific siRNAs were verified by western blot analysis as shown in Figure 5B, C and D respectively). The amount of cytoplasmic luciferase mRNA was then quantified by RT–qPCR, normalized to the amount of GAPDH mRNA and plotted on the graphs presented in Figure 5E, F and G as relative mRNA amounts. As we published previously (25), we found that in cells transfected with a control siRNA, the presence of EB2 led to a strong increase (16 - to 27-fold) in the amount of Renilla luciferase mRNA (compare lane 2 to lane 1 in panels E, F and G). When we inhibited endogenous SRp20 expression with a specific siRNA, EB2 did not induce any increase in the amount of Renilla luciferase mRNA (compare lane 4 to lane 3 in panel E). However, it should be noted that depletion of SRp20, in the absence of EB2, induced a reproducible increase (on average 5-fold) in the amount of cytoplasmic Renilla luciferase mRNA (compare lane 3 to lane 1 in panel E). The results of concomitant quantification of Renilla luciferase nuclear mRNAs (Supplementary Figure S1) were very similar to those obtained with the cytoplasmic mRNAs: EB2 induced an increase in the amount of nuclear luciferase RNA (10-fold). So did SRp20 depletion by itself (9-fold) and, in this case of SRp20 depletion, EB2 did not increase the amount of nuclear luciferase RNA. In fact, EB2 rather induced a diminution of nuclear luciferase RNA in the absence of SRp20. This effect of SRp20 depletion on both the amount of nuclear and cytoplasmic Renilla luciferase RNA, suggests that SRp20 targets this specific mRNA and either induces its destabilization or stimulates cryptic splicing, which eliminates part of the luciferase mRNA sequence, including that amplified in our RT–PCR reaction.

Inhibition of either 9G8 or SF2/ASF expression (Figure 5C and D respectively) also affected EB2-mediated cytoplasmic accumulation of Renilla luciferase mRNA, although to a much lower extent. Moreover, in the absence of EB2, depletion of either 9G8 or SF2/ASF did not have any noticeable impact on the level of the Renilla luciferase mRNA (Figure 5F and G). The results of concomitant quantification of the nuclear Renilla luciferase RNAs fully mimicked the results of the quantification obtained with the cytoplasmic mRNAs (data not shown).

Taken together, these results strongly suggest that SR proteins—and in the case of this specific mRNA, in particular SRp20—are required for efficient EB2-dependent cytoplasmic accumulation of its target mRNAs.

EB2 induces efficient cytoplasmic accumulation of human β-globin cDNA transcript in a SRp20-dependent manner

In the Renilla luciferase mRNA model, SRp20 appears to be the main SR protein necessary for EB2-dependent

cytoplasmic accumulation of the mRNA. SRp20 could be necessary, either for the efficient recruitment/stabilization of EB2 to the RNA or on the contrary, SRp20 could be recruited/stabilized onto the RNA by EB2 and participate actively in the stabilization and export of the mRNP. Interestingly, Huang and Steitz previously demonstrated that SRp20 (and 9G8) interacts specifically with a 22-nt RNA element from the mouse histone *H2a* gene (Figure 6A) (4). Insertion of this 22-nt motif, upstream of the human β-globin cDNA sequence in reporter construct β1(−)2(−) (Figure 6B) inhibits cryptic splicing between the β-globin-coding sequence and vector sequences, improves polyadenylation efficiency and enhances nuclear export. These effects increased with the number of tandemly repeated copies of the 22-nt element in a synergistic manner (4). We thus took advantage of these reporter constructs to study the effect of EB2 in relation to the presence of well-identified SRp20/9G8-binding sites. The constructs depicted in Figure 6B were thus used in transient transfections, either alone or together with an expression plasmid for EB2. Cytoplasmic RNA was then isolated and analysed by RT–PCR. As expected from the previous results of Huang and Steitz (4), we observed that the amount of cytoplasmic β-globin mRNA increased with the multimerization of the 22-nt motif (Figure 6C, lanes 1, 3, 5 and 7). Interestingly, although EB2 increased the amount of cytoplasmic β-globin mRNA expressed from the four β-globin constructs (Figure 6C, lane 2), we observed that this effect was inversely proportional to the number of 22-nt motifs present in the reporter constructs (Figure 6C, lanes 2, 4, 6 and 8 and Figure 6D).

We then asked whether the effect of EB2 on the β1(−)2(−) RNA was dependent on SRp20 by reiterating the above experiments in the presence of an anti-SRp20 siRNA or a control siRNA. The data presented in Figure 7, show that the EB2-induced increase in the cytoplasmic accumulation of the β-globin mRNAs expressed from the β1(−)2(−) construct, is strongly dependent on the presence of SRp20. Similarly to what we observed with the Renilla luciferase mRNA, we noted a reproducible increase in the amount of cytoplasmic β-globin mRNA when the cells were depleted of SRp20. This was not due to an indirect effect on the level of transcription initiated at the β-globin promoter since we did not observe any difference in the amount of transcripts generated from the 4×-βG construct that contains the 22-nt 'stabilizing' motif (data not shown). We also tested the impact of depleting the cells of either 9G8 or SF2/ASF by siRNA. Similarly to what was observed with the luciferase mRNA, the data, presented in Supplementary Figure S2, show a reproducible diminution of the EB2-dependent cytoplasmic accumulation of the β-globin mRNA upon depletion of 9G8 or SF2/ASF. However, the impact of these depletions on EB2's capacity to induce accumulation of these mRNAs in the cytoplasm is not as drastic as that of SRp20.

Taken together, these data suggest that the effect of EB2 on the cytoplasmic accumulation of the β-globin mRNA is highly dependent on the presence of SRp20 but that rather than being recruited onto the mRNA by

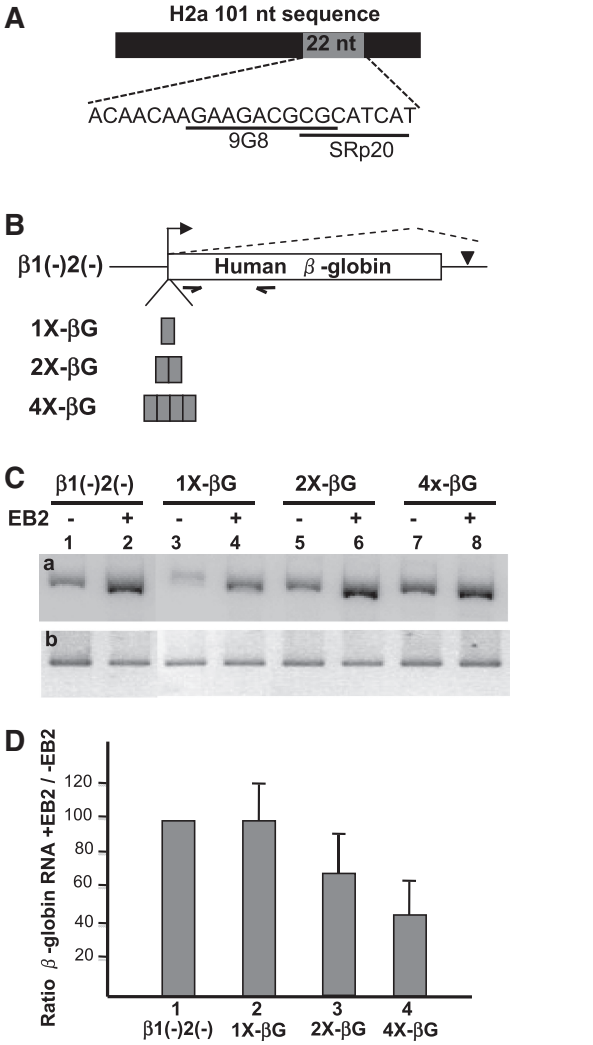

Figure 6. Effect of EB2 on the cytoplasmic accumulation of a human β-globin transcript that carries SRp20-binding sites. (**A**) Schematic representation of the mouse histone H2a 22-nt element. The black rectangle represents the 101-nt sequence from the mouse histone H2a found to facilitate cytoplasmic accumulation of intronless gene transcripts (47). The 22-nt element is shown with the 9G8 and SRp20-binding sites underlined. (**B**) Reporter constructs used for measuring the effect of EB2 in transient transfection experiments. The large open rectangle represent the human β-globin cDNA sequence, the black triangle the β-globin polyadenylation signal. An example of cryptic splicing from the human β-globin-coding region to the vector sequence is indicated. The grey boxes represent copies of the 22-nt element inserted at the beginning of the β-globin open reading frame. The two half arrows indicate the oligonucleotides used for RT–PCR amplifications. (**C**) Autoradiogram of an example of RT–PCR amplification of human β-globin RNAs expressed in transfected cells. The human β-globin plasmids depicted in C were transfected individually into HeLa cells either alone or together with an expression plasmid for EB2 as indicated. Forty-eight hours later, cytoplasmic RNAs were prepared and subjected to RT–PCR using the primer pair indicated in B (panel a) or a primer pair specific for β-actin mRNA as internal control (panel b). (**D**) Quantification of the results of three experiments. Each band from an experiment similar to that presented in C was quantified by using a PhosphorImager. The data are expressed as a ratio between the amount of cytoplasmic β-globin RNA measured in the presence of EB2 and the amount of cytoplasmic β-globin RNA measured in the absence of EB2. The error bars represent standard deviation.

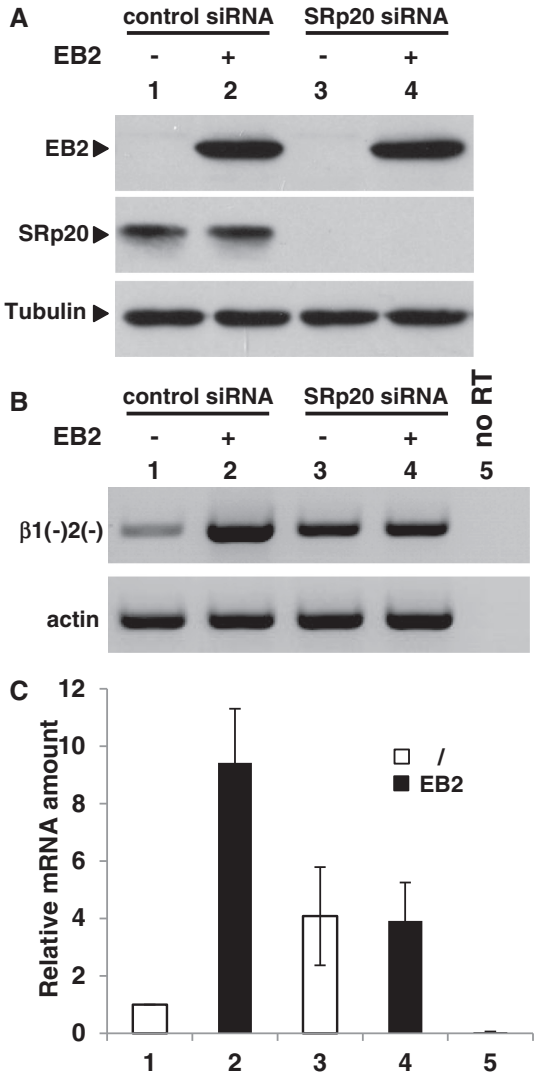

Figure 7. SRp20 is required for the EB2-dependent cytoplasmic accumulation of human β-globin cDNA transcripts. (**A**) Immunoblots of HeLa cells co-transfected with the β1(−)2(−) reporter construct together with an EB2 expression plasmid as indicated in the figure. Cells were previously transfected with either a control siRNA (lanes 1 and 2) or a siRNA specific for SRp20 (lanes 3 and 4). The blots were probed with either a M2-Flag mAb to detect tagged Flag-EB2, an anti-SRp20 mAb or an anti-α-Tubulin as a control of total protein amounts. (**B**) Autoradiogram of an example of RT–PCR amplifications of human β-globin RNAs expressed in cells tranfected as indicated in A, using the primer pair specific for human β-globin RNA (top panel) or a primer pair specific for actin RNA as internal control (bottom panel). (**C**) Quantification of the results of three experiments using a PhosphorImager. The error bars represent standard deviation.

specifically bound-SRp20, EB2 might mimic the effect of the 22-nt element by recruiting/stabilizing SRp20 onto the β-globin mRNA.

EB2 increases SRp20 recruitment onto human β-globin RNA

In order to test our above hypothesis that EB2 increases SRp20's binding to β-globin RNA, we performed RNA-immunoprecipitation experiments. For this, HeLa cells, transiently transfected with the β1(−)2(−) reporter construct either alone or together with increasing amounts of an expression vector for EB2, were UV-irradiated to crosslink proteins to the RNA. SRp20-containing complexes were then immunoprecipitated with a specific anti-SRp20 antibody and RNA prepared from these immunoprecipitated fractions was analysed by RT–PCR. As can be seen in Figure 8A, the amount of β1(−)2(−) RNA co-immunoprecipitated with SRp20 increased proportionally with the amount of EB2 expressed in the cells. We also performed RNA-immunoprecipitation experiments using an anti-Flag antibody to immunoprecipitate Flag tagged-EB2 in the presence or absence of SRp20. Figure 8B shows that the amount of β-globin RNA associated with EB2 remains unchanged when cells are depleted of SRp20. Taken together, these results indicate that EB2 bound to β-globin mRNA either recruits SRp20 onto the RNA or stabilizes SRp20's association with this mRNA.

EB2 counteracts the deleterious effect of SRp20 on cytoplasmic accumulation of EBV late viral mRNAs

Since SRp20 has such a drastic effect on two model mRNAs that depend on EB2 for their efficient accumulation in the cytoplasm, we tested whether depletion of SRp20 also affected the EB2-dependent cytoplasmic accumulation of specific viral mRNAs. We have previously shown that the late BDLF1 and BFRF3 mRNAs are very poorly expressed following induction of the productive cycle of a recombinant EBV lacking the EB2-coding gene (18). We thus cloned these two genes under the control of the CMV promoter into a plasmid lacking intronic sequences (plasmids pCI-FlagBDLF1-i and pCI-FlagBFRF3-i respectively) (Figure 9A). These two constructs were transfected into HeLa cells together (or not) with an expression plasmid for EB2. Cells were previously transfected with either a SRp20-specific siRNA or a control siRNA. Cytoplasmic RNAs were purified and analysed by semi-quantitative RT–PCR (Figure 9B). As expected, the level of both BFRF3 and BDLF1 mRNAs were drastically increased in the presence of EB2 (compare lanes 2 to lanes 1 of each panel). Interestingly, SRp20 depletion also drastically enhanced the level of both BFRF3 and BDLF1 (compare lanes 3 to lanes 1 of each panel) and the presence of EB2 had only a minimal (or no) additive effect in the absence of SRp20. Nuclear RNAs were also quantified in these experiments and the results always mimicked what was seen in the cytoplasm (data not shown), indicating that the low level of cytoplasmic mRNA detected in the presence of SRp20 but in the absence of EB2 was not due to an accumulation of these mRNAs in the nucleus. These data strongly suggest that the main effect of EB2 is to counteract a deleterious effect of SRp20 on intronless viral mRNAs.

In order to investigate the role of SRp20 during the replicative cycle of EBV, we used the $HEK293_{EBV}$ cell line. $HEK293_{EBV}$ cells carry an EBV recombinant that constitutively expresses the Green Fluorescent Protein (GFP). The replicative cycle of the virus can be activated in these cells by ectopic expression of the immediate early EBV transactivator EB1 (also called Zta or zebra).

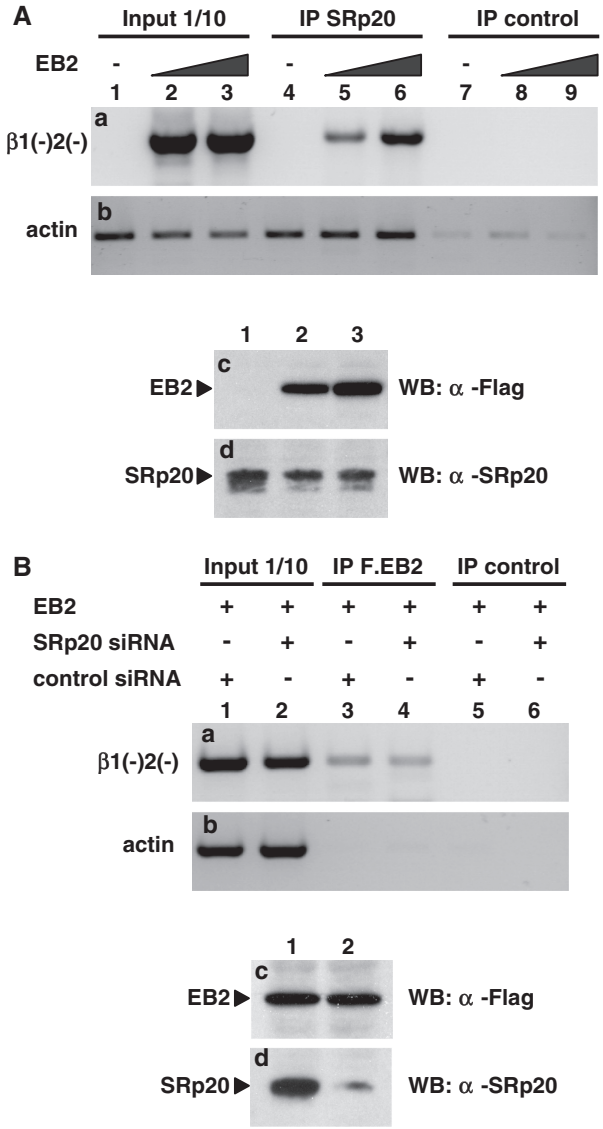

Figure 8. β-globin RNA-immunoprecipitation by anti-EB2 and anti-SRp20 antibodies. (**A**) HeLa cells were transfected with the β1(−)2(−) reporter construct together with increasing amounts (0, 0.5 or 1 μg) of Flag-tagged EB2 expression plasmid. After UV treatment of the cells, SRp20 containing complexes were immunoprecipitated using the anti-SRp20 mAb 7B4. RNA was then purified and the amount of specific β1(−)2(−) transcripts (panel a) or actin control mRNAs (panel b) co-immunoprecipitated was evaluated by semi-quantitative RT–PCR. The respective amounts of EB2 (panel c) and SRp20 (panel d) present in the samples used in the RNA-immunoprecipitations were evaluated by western blot analysis. (**B**) HeLa cells were transfected with the β1(−)2(−) reporter construct together with a Flag-tagged EB2 expression plasmid after transfection of the cells with an anti-SRp20 siRNA or a control siRNA as indicated. After UV treatment of the cells, EB2-containing complexes were immunoprecipitated using an anti-Flag M2 antibody. RNA was then purified and the amount of specific β1(−)2(−) transcripts (panel a) or actin control mRNA (panel b) co-immunoprecipitated was evaluated by semi-quantitative RT–PCR. The respective amounts of EB2 (panel c) and SRp20 (panel d) present in the samples used in the RNA-immunoprecipitations were evaluated by western blot analysis.

The amount of virus produced is then quantified following infection of Raji cells, by counting the number of GFP-expressing cells (43). We thus transfected $HEK293_{EBV}$ cells with a SRp20-specific siRNA or a control siRNA prior to transfection with the EB1 expression plasmid. As shown Figure 9C, virus production from cells in which SRp20 is down-regulated was reproducibly higher. This effect of SRp20 depletion on virus production was not unexpected since we have shown above, in the case of the two late viral mRNA, BDLF1 and BFRF3, that SRp20 depletion itself induced the cytoplasmic accumulation of these two mRNAs, even in the absence of EB2. In accordance with these results, over-expression of SRp20 in $HEK293_{EBV}$ cells led to a diminution of virus production (data not shown). We then asked whether SRp20 depletion by itself could induce virus production in the absence of EB2. For this we repeated the above experiments with $HEK293_{EBV\text{-}BMLF1KO}$ cells that carry an EBV recombinant with the EB2-coding gene deleted (16). The results shown Figure 9D indicate that in the absence of EB2, SRp20 depletion was clearly not sufficient to increase virus production. It is interesting to note that when we trans-complemented the $HEK293_{EBV\text{-}BMLF1KO}$ cells depleted of SRp20 with an EB2 expression plasmid, we observed an increase in virus production very similar to that observed in the $HEK293_{EBV}$ cells treated with the SRp20 siRNA.

Taken together, these results suggest that one of the mechanisms by which EB2 stimulates the cytoplasmic accumulation of viral mRNAs is by counteracting the negative effect of SRp20 on these same mRNAs.

DISCUSSION

The EBV early protein, EB2, has been found to affect multiple cellular pathways involved in mRNA processing. It was thus interesting to better understand how EB2 interacts with the cellular network of proteins involved in mRNA processing. We approached this question by setting up a wide-scale yeast two-hybrid screen. Although probably not completely exhaustive, this screen allowed us to identify 42 putative cellular partners for EB2. Among these, only Sp100 (46) and RBM15b/OTT3 (21) had been previously described as being direct interactors of the viral protein. Sp100 is a component of PML bodies, which are disrupted upon EBV productive cycle reactivation (48). RBM15b/OTT3 directly interacts with NXF1 and acts at the post-transcriptional level to activate reporter gene expression (23). hnRNPC was previously found to be present in a complex with EB2, although no direct interaction was demonstrated (49). That we have now identified this protein in our Y2H screen argues for a direct interaction between hnRNPC and EB2. Interestingly, in our list of novel interactors, we found several proteins known for their implication in splicing (PUF60, SF3A2, SRSF1, SRSF3, SRSF7 and ZRSR2) including several members of the SR family of proteins. Previously, another member of the SR family, SFRS10, was also found to interact with EB2 in a yeast 2YH screen (46). Furthermore, SRp20

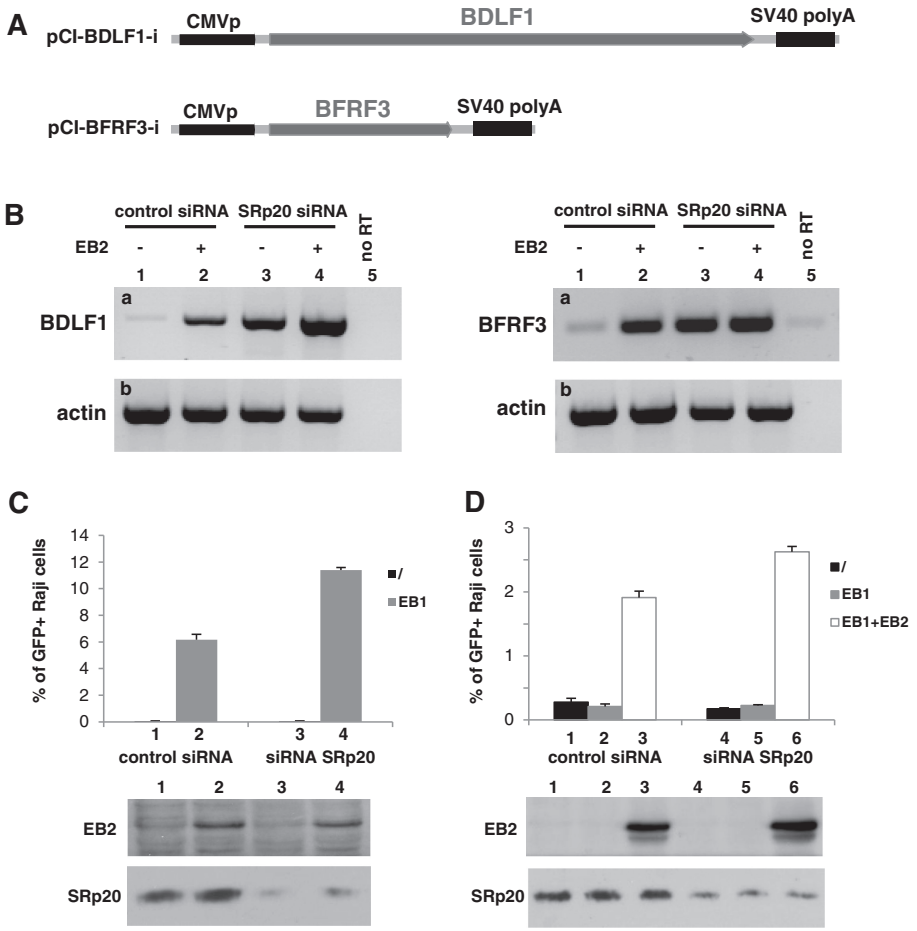

Figure 9. Impact of SRp20 depletion on the cytoplasmic accumulation of late viral mRNAs and on the production of virions. (**A**) Schematic representation of the pCI-BDLF1-i and pCI-BFRF3-i expression plasmids. (**B**) HeLa cells were co-transfected with pCI-BDLF1-i or pCI-BFRF3-i together or not with an EB2 expression plasmid. Cells were previously transfected with an anti-SRp20 siRNA or a control siRNA as indicated. Twenty-four hours later, cytoplasmic RNAs were prepared and subjected to RT–PCR using primer pairs specific for BDLF1 and BFRF3 respectively (panels a) or a primer pair specific for β-actin mRNA as internal control (panels b). (**C**) The EBV replicative cycle was induced in $HEK293_{EBV}$ cells previously treated with a SRp20 siRNA or a control siRNA, by transfection of an EB1 (BZLF1) expression plasmid. Cells supernatant were recuperated 72 h later and used to infect Raji cells. The number of GFP-expressing Raji cells was then evaluated 72 h later by FACS analysis. The efficiency of EB2 expression and SRp20 depletion was evaluated by western analysis and shown in the lower panels. (**D**) The EBV replicative cycle was induced in $HEK293_{EBV\text{-}BMLF1KO}$ cells previously treated with a SRp20 siRNA or a control siRNA, by transfection of an EB1 (BZLF1) expression plasmid together or not with an expression plasmid for EB2. Cells supernatant were recuperated 48 h later and used to infect Raji cells. The number of GFP-expressing Raji cells was then evaluated 72 h later by FACS analysis. The efficiency of EB2 expression and SRp20 depletion was evaluated by western blot analysis and shown in the lower panels.

(SRSF3) was recently affinity purified in a complex with EB2 (27). The characterization of interactions between EB2 and several proteins involved in splicing was quite striking. Interestingly, these same three SR proteins were recently found to interact with IE4, the EB2 orthologue in varicella zoster (13) but the functional impact of these interactions was not studied. SRp20 also interacts with ICP27, the EBV orthologue in HSV1 (50). Both SRp20 and 9G8 co-localizes with ICP27 in HSV-infected cells and their down-regulation by use of specific siRNAs, reduces viral yields (51). However, the mechanisms by which SRp20 and 9G8 down-regulation exert this effect were not deciphered. We thus decided to study in more detail the interaction between EB2 and the three SR proteins identified in our screen.

We first confirmed the interaction between EB2 and the three SR proteins both by co-immunoprecipitation in mammalian cells and by GST–pull down. All experiments were realized in the presence of RNase showing that the interactions are RNA-independent. We also demonstrated the interaction in live cells, since over-expression of each of the three SR proteins is able to induce the nuclear re-localization of a cytoplasmic form of EB2 generated by mutating its two NLS (20). Although SF2/ASF, SRp20 and 9G8 are known to shuttle continuously between the nucleus and the cytoplasm (52) their apparent localization in cells is nuclear. EB2 is also a shuttling protein with a predominant nuclear localization: we previously showed that the cellular nuclear mRNA export protein NXF1 participates in the nuclear export

of EB2 by binding to an NES sequence present in its N-terminal (24). Moreover, we have mapped two nuclear localization sequences (NLS) rich in KR residues that are responsible for nuclear import (20). However, mutation of the two NLS sequences of EB2 was not sufficient to completely inhibit translocation of EB2 from the cytoplasm to the nucleus. Our new data suggests that the interaction of EB2 with the SR proteins could result in the active translocation of EB2 from the cytoplasm to the nucleus or in its retention in the nucleus.

One of the main functions of EB2 in the productive cycle of EBV is to stimulate the cytoplasmic accumulation of most of the early and late viral mRNAs whose particularity is to be expressed from intronless genes (16,18,53). We thus tested the importance of the interaction between EB2 and the SR proteins for the cytoplasmic accumulation of mRNA generated from intronless genes. For this, we used two different reporter models: the first is based on an intronless reporter construct coding for the Renilla luciferase. We previously found that EB2 stimulates both cytoplasmic accumulation of the mRNA transcribed from this construct and ensures its efficient translation (25). The second model is a reporter construct carrying the human β-globin cDNA (4). Interestingly, by using siRNA we found that SRp20 depletion induced an increase in the cytoplasmic accumulation of both mRNAs and that in this case of SRp20 depletion, EB2 did not increase further the amount of mRNA in the cytoplasm. Since depletion of either 9G8 or SF2/ASF had only limited effect in the same kind of experiments, we decided to focus on SRp20. Interestingly, we found that SRp20 affected in a very similar manner two EBV late mRNAs originated from the BFRF3 and BDLF1 genes respectively. In all cases, depletion of SRp20 by itself induced a strong accumulation of the mRNA in the cytoplasm and EB2 had no or little additive effect on the amount of cytoplasmic mRNA. It is also important to note that when we quantified the amount of nuclear RNA for these specific transcripts, we observed that their abundance is very low (at least 1/20th of the cytoplasmic RNA) and varies in the same proportions as that of their corresponding cytoplasmic RNA. These data suggest that SRp20 exerts a negative effect on the amount of each of the four transcripts we have analysed in this study. This effect is likely to be nuclear since SRp20 depletion affects the amount of nuclear RNA in the same way as the amount of cytoplasmic RNA. In this context, it appears that one of the main functions of EB2 is to counteract this negative effect of SRp20.

How SRp20 so drastically induces a diminution of these four different mRNA species is still under study. However, several mechanisms can be invoked, such as induction of usage of cryptic splice sites, leading to the elimination of part of the original RNA, which renders the RNA undetectable by our PCR amplification, or destabilization of the mRNA. Our preliminary data suggest that both mechanisms could be involved in this effect of SRp20 (unpublished data).

The way EB2 counteracts these negative effects of SRp20 is still speculative but the data presented in this study by using a reporter construct carrying the human β-globin cDNA as a model, support the idea that by interacting with SRp20-specific mRNA targets, EB2 stabilizes SRp20 onto the mRNA. In effect, by using RNA-immunoprecipitations, we found that EB2 induced an increase association of SRp20 with the β-globin transcript. Interestingly, it was previously shown (4,54), that the RNA synthesized from this construct is inefficiently polyadenylated and poorly exported to the cytoplasm. Furthermore, cryptic splicing between the β-globin-coding sequence and vector sequences also contributed to lower the global amount of β-globin mRNA. The introduction in this construct of several copies of the mouse histone H2a 22-nt sequence that is specifically bound by the SR proteins, SRp20 or 9G8, was shown to promote inhibition of cryptic splicing and to enhance polyadenylation and nuclear export (4). By recruiting or stabilizing a direct interaction of SRp20 onto the β-globin mRNA, EB2 would appear to mimic the effect of the multimerized 22-nt element. SR protein-binding sites are largely degenerated and difficult to predict. Interestingly, wide-scale analyses have recently shown that SRp20 associates *in vivo* with a great number of mRNAs, including intronless mRNAs (55,56). Thus, SRp20 might interact at low affinity with several non-repertoriated sites on the β-globin mRNA. EB2 bound to the β-globin mRNA would then stabilize SRp20's association to this RNA resulting in a better polyadenylation of the transcript and inhibition of cryptic splicing. Furthermore, both SRp20 and EB2 can directly interact with NXF1 and thus lead to efficient nuclear export of their associated mRNPs (24,57).

In this study, we have described a mechanism by which EB2 recruits/stabilizes SR proteins onto mRNA generated from intronless genes. Since SR proteins are known for their role in both constitutive and alternative splicing, this suggests that EB2 might interfere with cellular mRNA splicing. Indeed, we have previously shown in different models that EB2 favours cytoplasmic accumulation of un-spliced mRNA with respect to spliced mRNAs generated from the same gene, especially when the spliced mRNAs are generated via cryptic splice sites, as is the case for the β-thalassemia gene (58). Moreover, Verma *et al*. (26) have recently shown that EB2 modulates the splicing of various cellular genes, including STAT1. In the case of STAT1, EB2 appears to change the ratio between two functionally distinct isoforms of STAT1 generated by alternative splicing (59) and SRp20 has been found to be involved in this modulation of STAT1 alternative splicing by EB2 (27). Whether this effect on cellular genes is important for EBV's replication remains to be demonstrated.

Given the drastic effect of SRp20 depletion on several EB2-target mRNAs, including two late EBV mRNAs, we were of course interested in evaluating the effect of SRp20 depletion on the EBV replicative cycle itself. However, since one of the functions of EB2 is to counteract the negative effect of SRp20 on the accumulation of specific mRNA targets, we could expect that SRp20 depletion, in the presence of EB2, might not have any effect at all, which is exactly what we observed. In fact, we even observed a slight but reproducible increase in virus

production when SRp20 was down-regulated. In accordance, over-expression of SRp20 slightly diminished virus production (unpublished observations). It is interesting to note that SRp20 depletion has a very different impact on the EBV and HSV replicative cycle respectively since in HSV-infected cells SRp20 down-regulation was found to reduce viral yields (51). These results confirm once again that although these two orthologues are both necessary for the efficient cytoplasmic accumulation of their respective viral mRNAs, their mechanisms of action are clearly different which explains that ICP27 cannot trans-complement an EB2 compromised EBV recombinant (16).

By using cells infected by a virus recombinant with the EB2-coding region deleted, we asked whether SRp20 depletion could by itself allow the production of viruses in the absence of EB2, which was not the case. Again, this result was not unexpected since EB2 has also been reported to stimulate translation of its target mRNAs (25), which could be a limited step for the progression of the viral replicative cycle. Furthermore, although we have not as yet identified any, some of the early or late viral mRNAs might be more sensitive to a similar effect of other SR proteins. Interestingly, it has been recently shown that each SR protein accumulates *in vivo* on a distinct set of mRNAs (55,56). It is thus likely that SF2/ASF or 9G8 could fulfil the same function as SRp20 for EB2-mediated cytoplasmic accumulation of mRNA species other than those used in this study, depending on their pattern of association with different RNAs.

In conclusion we report here a novel mechanism by which the EBV protein EB2 favours the efficient accumulation of viral mRNAs generated from intronless genes by antagonizing the negative effect of SRp20 on these mRNAs.

SUPPLEMENTARY DATA

Supplementary Data are available at NAR Online: Supplementary Figures 1 and 2.

ACKNOWLEDGEMENTS

The authors thank Drs Y. Huang and J. A. Steitz for providing plasmids β1(−)2(−), 1X-βG, 2X-βG and 4X-βG. The authors acknowledge the contribution of the 'Genetic Analysis and Vectorology' platform (B. Blanquier) and the 'Platim' microscope facilities of the SFR Biosciences Gerland-Lyon Sud (US8/UMS3444). Finally, the authors thank Dr R. Buckland for reading the manuscript.

FUNDING

Institut National de la Santé et de la Recherche Médicale (INSERM); Agence Nationale pour la Recherche [RPV06120CSA and RPV09056CSA to E.M.]; Pôle de Compétitivité Lyon-Biopôle; and Cluster de Recherche Rhône-Alpes en Infectiologie. Q.B. is recipient of a fellowship from the Ministère de la Recherche et de la Technologie (MRT) and of Association pour la Recherche sur le Cancer. F.J. is the recipient of a fellowship from the Ministère de la Recherche et de la Technologie (MRT) and the Fondation pour la Recherche Médicale (FRM); E.M. is a CNRS scientist. Funding for open access charge: INSERM.

Conflict of interest statement. None declared.

REFERENCES

1. Iglesias,N. and Stutz,F. (2008) Regulation of mRNP dynamics along the export pathway. *FEBS Lett*., **582**, 1987–1996.
2. Stutz,F., Bachi,A., Doerks,T., Braun,I.C., Séraphin,B., Wilm,M., Bork,P. and Izaurralde,E. (2000) REF, an evolutionary conserved family of hnRNP-like proteins, interacts with TAP/Mex67p and participates in mRNA nuclear export. *RNA*, **6**, 638–650.
3. Cheng,H., Dufu,K., Lee,C.S., Hsu,J.L., Dias,A. and Reed,R. (2006) Human mRNA export machinery recruited to the 5' end of mRNA. *Cell*, **127**, 1389–1400.
4. Huang,Y. and Steitz,J.A. (2001) Splicing factors SRp20 and 9G8 promote the nucleocytoplasmic export of mRNA. *Mol. Cell*, **7**, 899–905.
5. Huang,Y., Gattoni,R., Stévenin,J. and Steitz,J.A. (2003) SR splicing factors serve as adapter proteins for TAP-dependent mRNA export. *Mol. Cell*, **11**, 837–843.
6. Nojima,T., Hirose,T., Kimura,H. and Hagiwara,M. (2007) The interaction between cap-binding complex and RNA export factor is required for intronless mRNA export. *J. Biol. Chem*., **282**, 15645–15651.
7. Chen,I.H., Li,L., Silva,L. and Sandri-Goldin,R.M. (2005) ICP27 recruits Aly/REF but not TAP/NXF1 to herpes simplex virus type 1 transcription sites although TAP/NXF1 is required for ICP27 export. *J. Virol*., **79**, 3949–3961.
8. Koffa,M., Clements,J., Izaurralde,E., Wadd,S., Wilson,S., Mattaj,I. and Kuersten,S. (2001) Herpes simplex virus ICP27 protein provides viral mRNAs with access to the cellular mRNA export pathway. *EMBO J*., **20**, 5769–5778.
9. Lischka,P., Toth,Z., Thomas,M., Mueller,R. and Stamminger,T. (2006) The UL69 transactivator protein of human cytomegalovirus interacts with DEXD/H-Box RNA helicase UAP56 to promote cytoplasmic accumulation of unspliced RNA. *Mol. Cell. Biol*., **26**, 1631–1643.
10. Malik,P., Blackbourn,D.J. and Clements,B. (2004) The evolutionarily conserved Kaposi's sarcoma-associated herpesvirus ORF57 protein interacts with REF protein and acts as an RNA export factor. *J. Biol. Chem*., **279**, 33001–33011.
11. Boyne,J.R., Colgan,K.J. and Whitehouse,A. (2008) Recruitment of the complete hTREX complex is required for Kaposi's sarcoma-associated herpesvirus intronless mRNA nuclear export and virus replication. *PLoS Pathog*., **4**, e1000194.
12. Williams,B.J., Boyne,J.R., Goodwin,D.J., Roaden,L., Hautbergue,G.M., Wilson,S.A. and Whitehouse,A. (2005) The prototype gamma-2 herpesvirus nucleocytoplasmic shuttling protein, ORF 57, transports viral RNA through the cellular mRNA export pathway. *Biochem. J*., **387**, 295–308.
13. Ote,I., Lebrun,M., Vandevenne,P., Bontems,S., Medina-Palazon,C., Manet,E., Piette,J. and Sadzot-Delvaux,C. (2009) Varicella-zoster virus IE4 protein interacts with SR proteins and exports mRNAs through the TAP/NXF1 pathway. *PLoS One*, **4**, e7882.
14. Farjot,G., Buisson,M., Duc Dodon,M., Gazzolo,L., Sergeant,A. and Mikaelian,I. (2000) Epstein-Barr virus EB2 protein exports unspliced RNA via a Crm-1-Independent pathway. *J. Virol*., **74**, 6068–6076.
15. Semmes,O.J., Chen,L., Sarisky,R.T., Gao,Z., Zhong,L. and Hayward,S.D. (1998) Mta has properties of an RNA export protein and increases cytoplasmic accumulation of Epstein-Barr virus replication gene mRNA. *J. Virol*., **72**, 9526–9534.
16. Gruffat,H., Batisse,J., Pich,D., Neuhierl,B., Manet,E., Hammerschmidt,W. and Sergeant,A. (2002) Epstein-Barr virus

mRNA export factor EB2 is essential for production of infectious virus. *J. Virol.*, **76**, 9635–9644.
17. Hiriart,E., Bardouillet,L., Manet,E., Gruffat,H., Penin,F., Montserret,R., Farjot,G. and Sergeant,A. (2003) A region of the Epstein-Barr virus (EBV) mRNA export factor EB2 containing an arginine-rich motif mediates direct binding to RNA. *J. Biol. Chem.*, **278**, 37790–37798.
18. Batisse,J., Manet,E., Middeldorp,J., Sergeant,A. and Gruffat,H. (2005) Epstein-Barr virus mRNA export factor EB2 is essential for intranuclear capsid assembly and production of gp350. *J. Virol.*, **79**, 14102–14111.
19. Han,Z., Marendy,E., Wang,Y.D., Yuan,J., Sample,J.T. and Swaminathan,S. (2007) Multiple roles of Epstein-Barr virus SM protein in lytic replication. *J. Virol.*, **81**, 4058–4069.
20. Hiriart,E., Farjot,G., Gruffat,H., Nguyen,M.V., Sergeant,A. and Manet,E. (2003) A novel nuclear export signal and a REF interaction domain both promote mRNA export by the Epstein-Barr virus EB2 protein. *J. Biol. Chem.*, **278**, 335–342.
21. Hiriart,E., Gruffat,H., Buisson,M., Mikaelian,I., Keppler,S., Meresse,P., Mercher,T., Bernard,O.A., Sergeant,A. and Manet,E. (2005) Interaction of the Epstein-Barr virus mRNA export factor EB2 with human Spen proteins SHARP, OTT1, and a novel member of the family, OTT3, links Spen proteins with splicing regulation and mRNA export. *J. Biol. Chem.*, **280**, 36935–36945.
22. Lindtner,S., Zolotukhin,A.S., Uranishi,H., Bear,J., Kulkarni,V., Smulevitch,S., Samiotaki,M., Panayotou,G., Felber,B.K. and Pavlakis,G.N. (2006) RNA-binding motif protein 15 binds to the RNA transport element RTE and provides a direct link to the NXF1 export pathway. *J. Biol. Chem.*, **281**, 36915–36928.
23. Uranishi,H., Zolotukhin,A.S., Lindtner,S., Warming,S., Zhang,G.M., Bear,J., Copeland,N.G., Jenkins,N.A., Pavlakis,G.N. and Felber,B.K. (2009) The RNA-binding motif protein 15B (RBM15B/OTT3) acts as cofactor of the nuclear export receptor NXF1. *J. Biol. Chem.*, **284**, 26106–26116.
24. Juillard,F., Hiriart,E., Sergeant,N., Vingtdeux-Didier,V., Drobecq,H., Sergeant,A., Manet,E. and Gruffat,H. (2009) Epstein-Barr virus protein EB2 contains an N-terminal transferable nuclear export signal that promotes nucleocytoplasmic export by directly binding TAP/NXF1. *J. Virol.*, **83**, 12759–12768.
25. Ricci,E.P., Mure,F., Gruffat,H., Decimo,D., Medina-Palazon,C., Ohlmann,T. and Manet,E. (2009) Translation of intronless RNAs is strongly stimulated by the Epstein-Barr virus mRNA export factor EB2. *Nucleic Acids Res.*, **37**, 4932–4943.
26. Verma,D. and Swaminathan,S. (2008) Epstein-Barr virus SM protein functions as an alternative splicing factor. *J. Virol.*, **82**, 7180–7188.
27. Verma,D., Bais,S., Gaillard,M. and Swaminathan,S. (2010) Epstein-Barr virus SM protein utilizes cellular splicing factor SRp20 to mediate alternative splicing. *J. Virol.*, **84**, 11781–11789.
28. Shepard,P.J. and Hertel,K.J. (2009) The SR protein family. *Genome Biol.*, **10**, 242.
29. Long,J.C. and Caceres,J.F. (2009) The SR protein family of splicing factors: master regulators of gene expression. *Biochem. J.*, **417**, 15–27.
30. Sanford,J.R., Gray,N.K., Beckmann,K. and Caceres,J.F. (2004) A novel role for shuttling SR proteins in mRNA translation. *Genes Dev.*, **18**, 755–768.
31. Michlewski,G., Sanford,J.R. and Caceres,J.F. (2008) The splicing factor SF2/ASF regulates translation initiation by enhancing phosphorylation of 4E-BP1. *Mol. Cell*, **30**, 179–189.
32. Bedard,K.M., Daijogo,S. and Semler,B.L. (2007) A nucleo-cytoplasmic SR protein functions in viral IRES-mediated translation initiation. *EMBO J.*, **26**, 459–467.
33. Swartz,J.E., Bor,Y.C., Misawa,Y., Rekosh,D. and Hammarskjold,M.-L. (2007) The shuttling SR protein 9G8 plays a role in translation of unspliced mRNA containing a constitutive transport element. *J. Biol. Chem.*, **282**, 19844–19853.
34. Delecluse,H.J., Pich,D., Hilsendegen,T., Baum,C. and Hammerschmidt,W. (1999) A first-generation packaging cell line for Epstein-Barr virus-derived vectors. *Proc. Natl Acad. Sci. USA*, **96**, 5188–5193.
35. Walhout,A.J., Temple,G.F., Brasch,M.A., Hartley,J.L., Lorson,M.A., van den Heuvel,S. and Vidal,M. (2000) Tracing lifestyle adaptation in prokaryotic genomes. *Front Microbiol.*, **3**, 48.
36. Pellet,J., Tafforeau,L., Lucas-Hourani,M., Navratil,V., Meyniel,L., Achaz,G., Guironnet-Paquet,A., Aublin-Gex,A., Caignard,G., Cassonnet,P. *et al.* (2010) ViralORFeome: an integrated database to generate a versatile collection of viral ORFs. *Nucleic Acids Res.*, **38**, D371–D378.
37. Medina-Palazon,C., Gruffat,H., Mure,F., Filhol,O., Vingtdeux-Didier,V., Drobecq,H., Cochet,C., Sergeant,N., Sergeant,A. and Manet,E. (2007) Protein Kinase CK2 phosphorylation of EB2 regulates its function in the production of Epstein-Barr virus infectious viral particles. *J. Virol.*, **81**, 11850–11860.
38. Albers,M., Kranz,H., Kober,I., Kaiser,C., Klink,M., Suckow,J., Kern,R. and Koegl,M. (2005) Automated yeast two-hybrid screening for nuclear receptor-interacting proteins. *Mol. Cell Proteomics*, **4**, 205–213.
39. Tafforeau,L., Rabourdin-Combe,C. and Lotteau,V. (2012) Virus-Human Cell Interactomes. In: Suter,B. and Wanker,E.E. (eds), *Two Hybrid Technologies*. Springer Protocols, Humana Press, Springer.
40. Vidalain,P.O., Boxem,M., Ge,H., Li,S. and Vidal,M. (2004) Increasing specificity in high-throughput yeast two-hybrid experiments. *Methods*, **32**, 363–370.
41. Pellet,J., Meyniel,L., Vidalain,P.O., de Chassey,B., Tafforeau,L., Lotteau,V., Rabourdin-Combe,C. and Navratil,V. (2009) pISTil: a pipeline for yeast two-hybrid interaction sequence tags identification and analysis. *BMC Res. Notes*, **2**, 220.
42. Walhout,A.J. and Vidal,M. (2001) High-throughput yeast two-hybrid assays for large-scale protein interaction mapping. *Methods*, **24**, 297–306.
43. Delecluse,H.J., Hilsendegen,T., Pich,D., Zeidler,R. and Hammerschmidt,W. (1998) Propagation and recovery of intact, infectious Epstein-Barr virus from prokaryotic to human cells. *Proc. Natl Acad. Sci. USA*, **95**, 8245–8250.
44. Blaustein,M., Pelisch,F., Tanos,T., Muñoz,M.J., Wengier,D., Quadrana,L., Sanford,J.R., Muschietti,J.P., Kornblihtt,A.R., Cáceres,J.F. *et al.* (2005) Concerted regulation of nuclear and cytoplasmic activities of SR proteins by AKT. *Nat. Struct. Mol. Biol.*, **12**, 1037–1044.
45. Boyne,J.R. and Whitehouse,A. (2006) Nucleolar trafficking is essential for nuclear export of intronless herpesvirus mRNA. *Proc. Natl Acad. Sci. USA*, **103**, 15190–15195.
46. Calderwood,M.A., Venkatesan,K., Xing,L., Chase,M.R., Vazquez,A., Holthaus,A.M., Ewence,A.E., Li,N., Hirozane-Kishikawa,T., Hill,D.E. *et al.* (2007) Epstein-Barr virus and virus human protein interaction maps. *Proc. Natl Acad. Sci. USA*, **104**, 7606–7611.
47. Huang,Y. and Carmichael,G.G. (1997) The mouse histone H2a gene contains a small element that facilitates cytoplasmic accumulation of intronless gene transcripts and of unspliced HIV-1-related mRNAs. *Proc. Natl Acad. Sci. USA*, **94**, 10104–10109.
48. Bell,P., Lieberman,P.M. and Maul,G.G. (2000) Lytic but not latent replication of Epstein-Barr virus is associated with PML and induces sequential release of nuclear domain 10 proteins. *J. Virol.*, **74**, 11800–11810.
49. Key,S.C., Yoshizaki,T. and Pagano,J.S. (1998) The Epstein-Barr virus (EBV) SM protein enhances pre-mRNA processing of the EBV DNA polymerase transcript. *J. Virol.*, **72**, 8485–8492.
50. Sciabica,K.S., Dai,Q.J. and Sandri-Goldin,R.M. (2003) ICP27 interacts with SRPK1 to mediate HSV splicing inhibition by altering SR protein phosphorylation. *EMBO J.*, **22**, 1608–1619.
51. Escudero-Paunetto,L., Li,L., Hernandez,F.P. and Sandri-Goldin,R.M. (2010) SR proteins SRp20 and 9G8 contribute to efficient export of herpes simplex virus 1 mRNAs. *Virology*, **401**, 155–164.
52. Cáceres,J.F., Screaton,G.R. and Krainer,A.R. (1998) A specific subset of SR proteins shuttles continuously between the nucleus and the cytoplasm. *Genes Dev.*, **12**, 55–66.
53. Verma,D., Ling,C., Johannsen,E., Nagaraja,T. and Swaminathan,S. (2009) Negative autoregulation of EBV

replicative gene expression by Epstein-Barr virus (EBV) SM protein. *J. Virol.*, **83**, 8041–8050.
54. Huang,Y., Wimler,K.M. and Carmichael,G.G. (1999) Intronless mRNA transport elements may affect multiple steps of pre-mRNA processing. *EMBO J.*, **18**, 1642–1652.
55. Sapra,A.K., Ankö,M.L., Grishina,I., Lorenz,M., Pabis,M., Poser,I., Rollins,J., Weiland,E.M. and Neugebauer,K.M. (2009) SR protein family members display diverse activities in the formation of nascent and mature mRNPs in vivo. *Mol. Cell*, **34**, 179–190.
56. Ankö,M.L., Morales,L., Henry,I., Beyer,A. and Neugebauer,K.M. (2010) Global analysis reveals SRp20- and SRp75-specific mRNPs in cycling and neural cells. *Nat. Struct. Mol. Biol.*, **17**, 962–970.
57. Hargous,Y., Hautbergue,G.M., Tintaru,A.M., Skrisovska,L., Golovanov,A.P., Stevenin,J., Lian,L.Y., Wilson,S.A. and Allain,F.H. (2006) Molecular basis of RNA recognition and TAP binding by the SR proteins SRp20 and 9G8. *EMBO J.*, **25**, 5126–5137.
58. Buisson,M., Hans,F., Kusters,I., Duran,N. and Sergeant,A. (1999) The C-terminal region but not the Arg-X-Pro repeat of Epstein-Barr virus protein EB2 is required for its effect on RNA splicing and transport. *J. Virol.*, **73**, 4090–4100.
59. Ruvolo,V., Navarro,L., Sample,C.E., David,M., Sung,S. and Swaminathan,S. (2003) The Epstein-Barr virus SM protein induces STAT1 and interferon-stimulated gene expression. *J. Virol.*, **77**, 3690–3701.